Cell Reports

Article

Maternal progesterone and adipose mPRε in pregnancy regulate the embryonic nutritional state

Graphical abstract

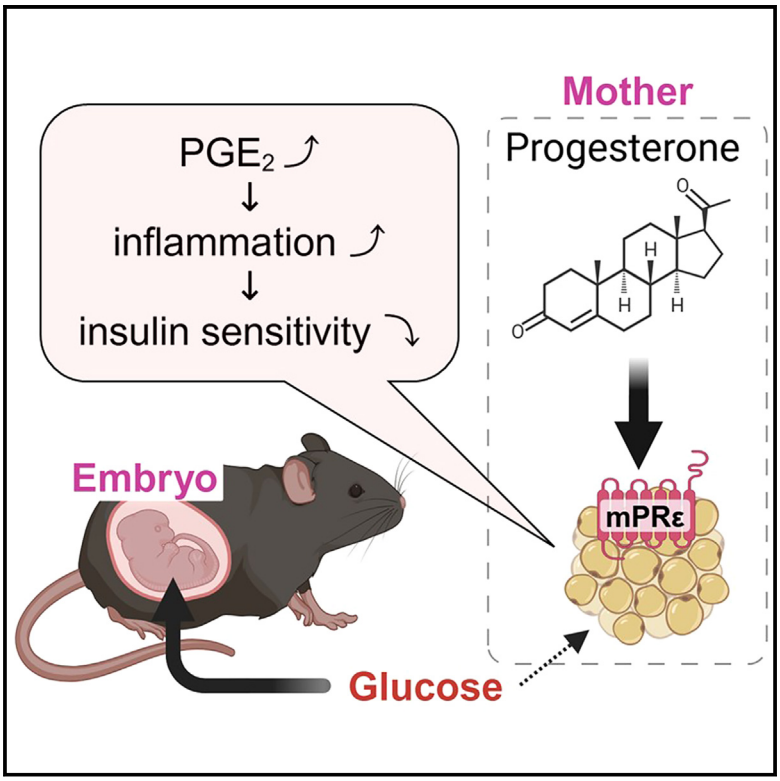

Authors

Keita Watanabe, Mayu Yamano, Junki Miyamoto, ..., Hiroaki Ohno, Eiji Kondoh, Ikuo Kimura

Correspondence

kimura.ikuo.7x@kyoto-u.ac.jp

In brief

Watanabe et al. demonstrate that high maternal progesterone during pregnancy supports efficient glucose supply to the developing embryo by increasing maternal insulin resistance via mPRε. This study suggests the potential use of mPRε modulators for managing pregnancy-related glycemic disorders such as gestational diabetes mellitus and for managing metabolic syndromes in offspring.

Highlights

- mPRε is abundant in adipose and mediates progesterone-induced insulin resistance
- mPRε deficiency disrupts glycemic control, causing metabolic disorder in offspring
- Progesterone-activated mPRε in WAT promotes arachidonate release and PGE_2 production

Watanabe et al., 2025, Cell Reports *44*, 115433
March 25, 2025
https://doi.org/10.1016/j.celrep.2025.115433

CellPress

Cell Reports

CellPress
OPEN ACCESS

Article

Maternal progesterone and adipose mPRε in pregnancy regulate the embryonic nutritional state

Keita Watanabe,[1,15] Mayu Yamano,[2,15] Junki Miyamoto,[3,15] Ryuji Ohue-Kitano,[4] Yuki Masujima,[1] Daiki Sasahara,[1,5] Yuki Mouri,[6] Nozomu Kono,[6] Shunsuke Inuki,[7] Fumitaka Osakada,[8,9,10] Kentaro Nagaoka,[10,11] Junken Aoki,[6,12] Yuki Sugiura,[13] Hiroaki Ohno,[7,10] Eiji Kondoh,[9,14] and Ikuo Kimura[1,2,10,12,16,*]

[1]Laboratory of Molecular Neurobiology, Graduate School of Biostudies, Kyoto University, Sakyo-ku, Kyoto 606-8501, Japan
[2]Department of Molecular Endocrinology, Graduate School of Pharmaceutical Sciences, Kyoto University, Sakyo-ku, Kyoto 606-8501, Japan
[3]Department of Applied Biological Science, Graduate School of Agriculture, Tokyo University of Agriculture and Technology, Fuchu, Tokyo 183-8509, Japan
[4]Department of Biological & Environmental Chemistry, Kindai University, 11-6 Kayanomori, Iizuka City, Fukuoka 820-8555, Japan
[5]Noster Inc., Kamiueno, Muko-shi, Kyoto 617-0006, Japan
[6]Graduate School of Pharmaceutical Sciences, University of Tokyo, 7-3-1, Hongo, Bunkyo-ku, Tokyo 113-0033, Japan
[7]Department of Bioorganic Medicinal Chemistry, Graduate School of Pharmaceutical Sciences, Kyoto University, Sakyo-ku, Kyoto 606-8501, Japan
[8]Laboratory of Cellular Pharmacology, Graduate School of Pharmaceutical Sciences, Nagoya University, Nagoya 464-8601, Japan
[9]Laboratory of Neural Information Processing, Institute for Advanced Research, Nagoya University, Nagoya 464-8601, Japan
[10]AMED-CREST, Japan Agency for Medical Research and Development, Chiyoda-ku, Tokyo 100-0004, Japan
[11]Laboratory of Veterinary Physiology, Graduate School of Agriculture, Tokyo University of Agriculture and Technology, Fuchu, Tokyo 183-8509, Japan
[12]Department of Moonshot Research and Development Program, Japan Science and Technology Agency, Chiyoda-ku, Tokyo 102-0076, Japan
[13]Center for Cancer Immunotherapy and Immunobiology, Kyoto University Graduate School of Medicine, Sakyo-ku, Kyoto 606-8501, Japan
[14]Department of Obstetrics and Gynecology, Faculty of Life Sciences, Kumamoto University, 1-1-1, Honjo, Chuo-Ku, Kumamoto City, Kumamoto 860-8556, Japan
[15]These authors contributed equally
[16]Lead contact
*Correspondence: kimura.ikuo.7x@kyoto-u.ac.jp
https://doi.org/10.1016/j.celrep.2025.115433

SUMMARY

Sex steroid hormones such as progesterone play a pivotal role in reproductive functions and maintaining pregnancy; however, the impact of progesterone on the interaction between mother and embryo is unclear. Here, we demonstrate that the relationship between maternal progesterone and membrane progesterone receptor epsilon (mPRε) in adipose tissue regulates embryonic nutritional environment and growth after birth in mice. The activation of adipose mPRε by increased progesterone during pregnancy enhances maternal insulin resistance via prostaglandin production, efficiently providing glucose to embryos. Correspondingly, the offspring of mPRε-deficient mothers exhibited metabolic dysfunction, whereas mPRε-deficient mothers with high-fat diet-induced obesity exhibited improved insulin sensitivity. These findings establish the importance of progesterone as a nutritional regulator between mother and embryo. Additionally, mPRε may represent a modulator for treating pregnant glycemic control disorders such as gestational diabetes mellitus, as well as metabolic syndrome in offspring.

INTRODUCTION

During the perinatal period, fetal growth is influenced by various maternal humoral factors that directly affect the development of various conditions/diseases, including allergies, neurological disorders, obesity, and diabetes.[1–5] For example, gestational diabetes mellitus[6] (i.e., glucose intolerance of variable degree caused by maternal overnutrition) and starvation due to maternal malnutrition[1–3] can lead to abnormal weights according to gestational age, posing a risk of excessive body weight gain and metabolic syndrome in offspring later in life.[7–12] Among maternal humoral factors, sex steroid hormones such as estrogen and progesterone are the most important for reproduction.[13–15] Their peak levels during pregnancy exceed 10 times those during the estrus cycle.[15,16] Therefore, maternal sex steroid hormones are considered crucial for maintaining pregnancy and embryonic

development. However, the underlying mechanisms and biological significance of maternal-embryonic crosstalk via these sex steroid hormones remain unclear.

In addition to reproductive functions, sex steroid hormones are involved in numerous physiological functions, including maternal behavior, aggression, emotion, feeding, circadian rhythm, sleep, and higher brain functions such as memory and learning.[13–16] Most of these hormones generate immediate responses that cannot be explained by nuclear receptors.[17,18] Instead, membrane progesterone receptors (mPRs) and G protein-coupled receptor (GPCR) 30, which are the respective membrane receptors for progesterone and estrogen,[19,20] may mediate the immediate physiological responses of sex steroid hormones, including activating mitogen-activated protein kinase (MAPK) signaling, increasing intracellular Ca^{2+}, and releasing fatty acids from membrane phospholipids.[17–21]

mPRε/PAQR9 belongs to the progestin and AdipoQ receptor (PAQR) family, which includes five unique mPR subtypes: mPRα/PAQR7, mPRβ/PAQR8, mPRγ/PAQR5, mPRδ/PAQR6, and mPRε.[22–24] mPRε can sense and respond to progesterone with half-maximal effective concentration (EC_{50}) values of approximately 13 nM[25,26]. Moreover, the progesterone-mPR signal participates in GPCR signaling and the MAPK cascade.[27] The physiological functions of hepatic mPRε include regulating fasting-induced ketogenesis and fatty acid oxidation,[28] whereas pancreatic mPRε contributes to glucose regulation and lipid homeostasis in diabetic mice.[29] However, the relationship between these phenotypes and progesterone as a ligand for mPRε remains unelucidated.

Considering the high expression of mPRε in white adipose tissue (WAT) and high levels of progesterone in pregnancy, the present study seeks to clarify the interaction between progesterone and adipose mPRε during pregnancy. Moreover, the mechanism(s) by which sex steroid hormones modulate the interaction between embryos and maternal metabolism is investigated using mPRε-deficient mice.

RESULTS

mPRε is abundantly expressed in adipose tissues

mPRε expression was assessed in adult mice on postnatal day 49 (P49), during sexual maturation, using quantitative real-time PCR. *mPRε* mRNA was detected in the liver, kidney, WAT, and brown adipose tissue (BAT) in males and females. Moreover, *mPRε* mRNA expression was significantly increased in the WATs of mice fed a high-fat diet (HFD) compared with those on normal chow (NC; Figure 1A). *mPRε* was the only mPR subtype expressed in the WATs of male and female mice (Figure 1B). Additionally, *mPRε* was only expressed in the mature adipocytes, not in the stromal vascular fraction (SVF); expression was significantly higher under HFD feeding than under NC feeding (Figure 1C). Moreover, *mPRε* expression gradually increased with adipogenesis of mouse embryonic fibroblasts (MEFs) in males and females (Figure 1D). Meanwhile, nuclear progesterone receptor (PGR) expression was observed only in the SVF of female WATs (Figure 1E). These findings suggest that *mPRε* is expressed in the adipocytes of WATs of male and female mice.

Progesterone exacerbates insulin resistance via mPRε

Next, mPRε-deficient mice were generated to clarify the physiological function of mPRε on energy metabolism (Figures S1A–S1C). In the HFD-induced obese mouse model, the body weights of mPRε-deficient mice did not differ significantly from those of wild-type (WT) mice in males or females during growth (Figure 2A). Similarly, the tissue weights and metabolic parameters in 16-week-old mice were comparable between WT and mPRε-deficient mice in males (Figures S2A–S2C) and females (Figures S2D–S2F). Plasma progesterone levels were below 10 nM (<EC_{50} of mPRε) in all mice (Figure 2B). In female mice, the corpus luteum degenerates after ovulation unless certain hormones are released.[30] Therefore, mPRε was externally stimulated via subcutaneously (s.c.) progesterone injection. This increased plasma progesterone levels (∼50 nM) in both males and females of WT and mPRε-deficient mice (Figure S3A). Moreover, progesterone injection exacerbated insulin resistance in male and female WT mice; however, this effect was abolished in male and female mPRε-deficient mice (Figures 2C–2F). Meanwhile, progesterone injection did not significantly impact plasma insulin levels between WT and mPRε-deficient mice (Figure S3B).

To clarify whether mPRε in WATs is responsible for the progesterone-induced effects, insulin signaling was analyzed using insulin-induced Akt phosphorylation and MEF-derived adipocytes. *mPRε* was the only mPR subtype expressed in the liver (Figure S3C) as well as WAT, whereas all mPR subtypes (mPRα/β/γ/δ/ε) were hardly expressed in muscles (Figure S3D). Progesterone injection also suppressed insulin-induced Akt phosphorylation in the WAT, not the liver or muscles, of WT mice (Figure 2G); however, this effect was not observed in the WAT of mPRε-deficient mice (Figure 2H). Additionally, adipocyte differentiation from MEFs, induced by a methylisobutylxanthine, dexamethasone, pioglitazone, and insulin cocktail,[31] did not differ significantly between WT and mPRε-deficient mice (Figure S3E). The influence of progesterone on adipogenesis was also comparable between WT and mPRε-deficient mice (Figure S3F). Although insulin-induced glucose uptake in MEF-induced adipocytes derived from WT mice was suppressed by progesterone, these effects were abolished in MEF-induced adipocytes derived from mPRε-deficient mice (Figure 2I). These findings suggest that progesterone-induced activation of mPRε in WATs promotes insulin resistance.

Maternal insulin resistance via mPRε provides nutrients to embryos

During pregnancy, there is an increase in maternal insulin resistance.[32] Given the substantial rise in maternal progesterone levels during pregnancy, the present study examined the insulin sensitivity of mPRε-deficient mice during pregnancy to clarify the relationship between progesterone and maternal insulin resistance. The progesterone levels of pregnant females (∼300 nM) were markedly higher than those of non-pregnant females (Figure 3A). Moreover, on gestational day 16.5 (GD16.5), mPRε-deficient female mice exhibited better insulin resistance than WT (Figure 3B). However, their plasma progesterone and insulin levels were comparable (Figures S4A and S4B). Although *mPRε* mRNA expression was comparable between

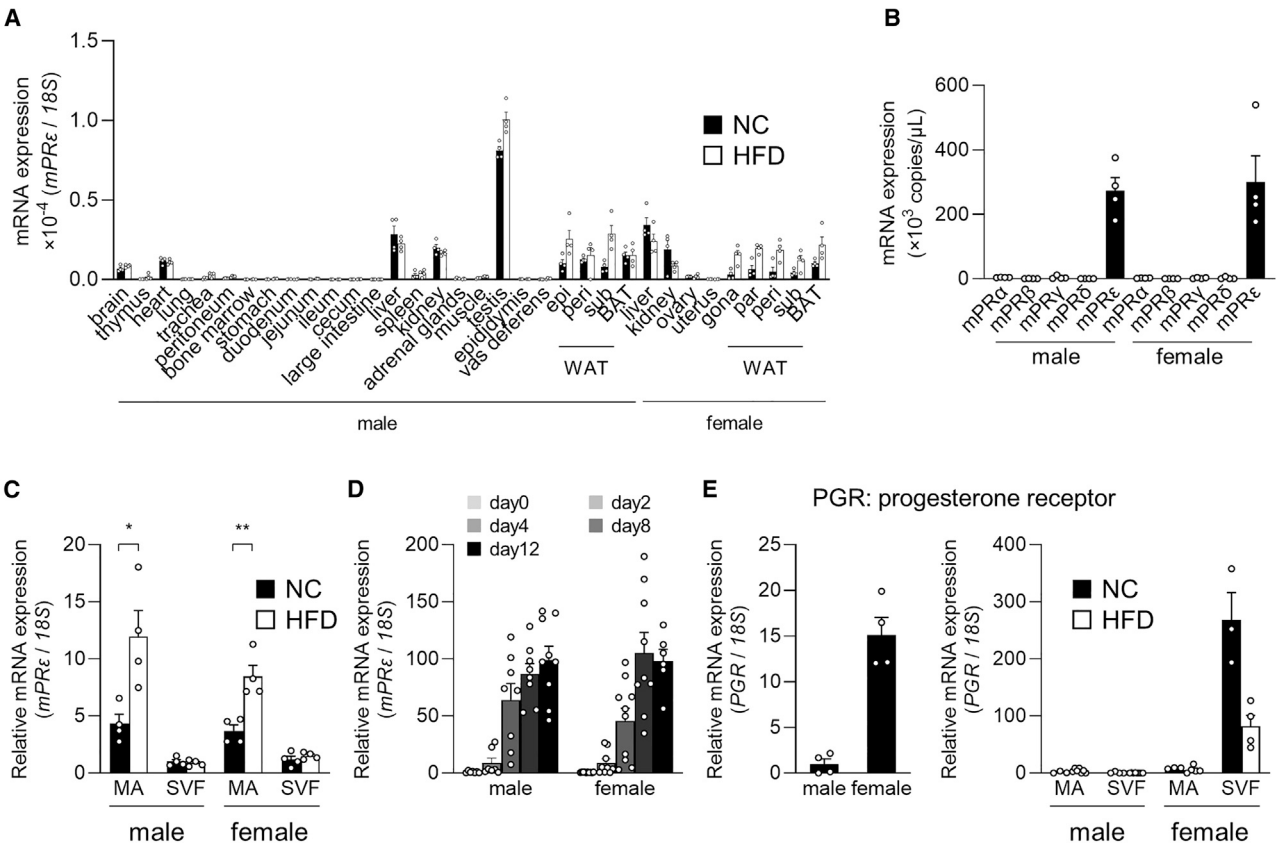

Figure 1. *mPRε* is sufficiently expressed in white adipose tissues

(A) *mPRε* mRNA expression in mouse tissues (postnatal day 49 [P49]) measured by quantitative real-time PCR (n = 3–4). BAT, brown adipose tissue; *18S* rRNA expression was used as the internal control. HFD, high-fat diet; NC, normal chow; WATs, white adipose tissues (epididymal adipose tissue).

(B) Expression of mPR subtypes in mouse WAT (n = 4; P49).

(C) *mPRε* expression in mature adipocytes (MA) and a stromal vascular fraction (SVF) of mice fed NC or HFD (n = 4). *$p < 0.05$; **$p < 0.01$ (Student's t test).

(D) *mPRε* mRNA expression in mouse embryonic fibroblast (MEF)-derived adipocytes during adipogenesis (n = 6–10).

(E) Expression of the nuclear progesterone receptor PGR in mouse WATs (left, n = 4). PGR expression in the MA and SVF of mice fed NC or HFD (right, n = 3–8; P49). Results are presented as mean ± standard error of the mean (SEM).

non-pregnant and GD16.5 female mice (Figure S4C), the blood glucose levels of mPRε-deficient GD16.5 female mice were significantly lower than those of WT GD16.5 female mice (Figure 3C). Similarly, the blood glucose levels of embryos in mPRε-deficient female mice were significantly lower than those of WT female mice (Figure 3C). Conversely, the insulin sensitivity of mPRε-deficient non-pregnant female mice was similar to that of WT non-pregnant female mice (Figure 3D).

Although the placenta influences fetal glucose and growth,[33] all mPR subtypes were hardly expressed in the placentas of GD16.5 female mice (Figure S5A). Progesterone levels in placenta were also similar between WT and mPRε-deficient GD16.5 female mice (Figure S5B). Consequently, RNA sequencing analysis in the placenta showed comparable gene expression between WT and mPRε-deficient GD16.5 female mice (Figures S5C and S5D). Additionally, insulin resistance was analyzed in a mouse model of HFD-induced gestational diabetes mellitus. Insulin resistance in WT GD16.5 female mice was markedly improved compared with in mPRε-deficient GD16.5 female mice (Figure 3E). Thus, mPRε-induced maternal insulin resistance during pregnancy enhances glucose availability for embryos.

mPRε deficiency in pregnancy causes postnatal growth abnormalities

The influence of maternal mPRε on offspring growth was investigated (Figure 4A). On P28, the body weights of both mPRε-deficient and heterozygous offspring from mPRε-deficient mothers were significantly lower than those of WT and heterozygous offspring from WT mothers (Figures 4B and S6A). The proportion of WATs was significantly lower in mPRε-deficient and heterozygous offspring from mPRε-deficient mothers than in WT and heterozygous offspring from WT mothers; however, there were no significant differences in all other tissue weights and lean mass between the groups (Figures S6A and S6B).

Moreover, mPRε-deficient offspring from two mPRε-deficient parents and WT offspring from two WT parents were fed an HFD during growth. Unlike mPRε-deficient offspring from two heterozygous parents (Figure 2A), the body weights of mPRε-deficient offspring from a mPRε-deficient mother were

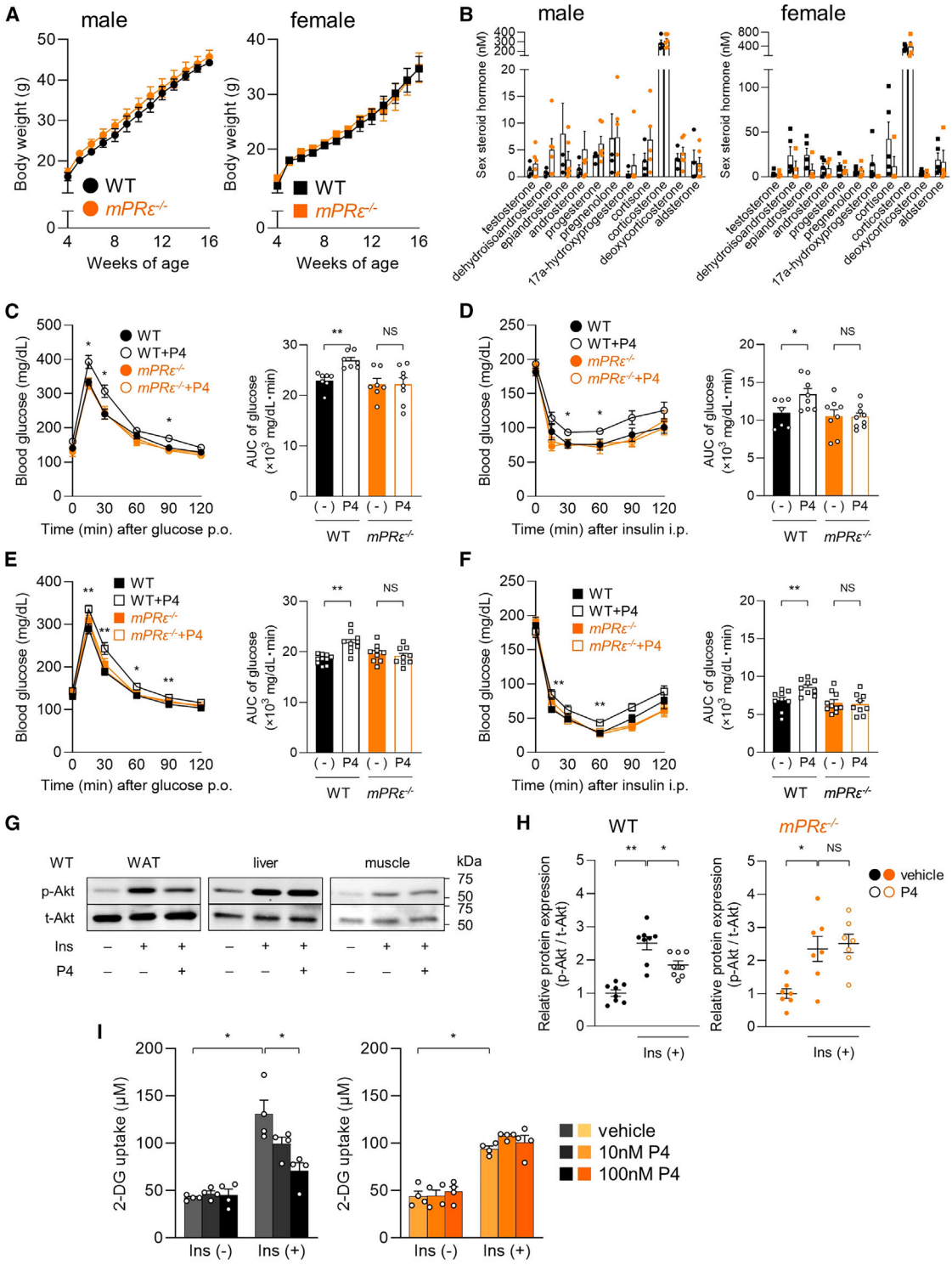

Figure 2. Progesterone enhances insulin resistance via adipose mPRε

(A) Changes in body weight of WT and *mPRε*$^{-/-}$ mice under HFD feeding (n = 4–6).

(B) Plasma steroid levels at 16 weeks of age (n = 4–6).

(C and E) Oral glucose tolerance test (OGTT) in male (C) or female (E) WT and *mPRε*$^{-/-}$ mice was performed at 15 min post-progesterone s.c. injection. n = 7–10; $^{*}p < 0.05$; $^{**}p < 0.01$ vs. WT (P4, progesterone).

(legend continued on next page)

significantly lower than those of WT offspring from a WT mother for both males and females during growth (Figure 4C). Similarly, the kidney and WAT weights of 16-week-old mPRε-deficient male offspring and the WAT weights of 16-week-old mPRε-deficient female offspring from mPRε-deficient mothers were also significantly lower than those of 16-week-old WT offspring from WT mothers (Figure 4D). Meanwhile, normalization of tissue weights by body weight revealed that the significant differences in kidneys, not WATs, were no longer present (Figures S6C and S6D). Therefore, metabolic dysfunction, including WATs, rather than growth retardation, may largely contribute to the observed phenotypes.

The levels of plasma triglycerides, non-esterified fatty acids (NEFAs), and total cholesterol in 16-week-old mPRε-deficient male offspring (Figure S7A) from mPRε-deficient mothers and the levels of plasma NEFAs and total cholesterol in 16-week-old mPRε-deficient female offspring (Figure S7D) from mPRε-deficient mothers were also sufficiently lower than those of WT offspring from WT mothers. Notably, the plasma insulin levels were significantly higher and lower in 16-week-old male and female offspring from mPRε-deficient mothers, respectively (Figures S7B and S7E), than in WT offspring from WT mothers. Furthermore, plasma progesterone levels were below 10 nM in male and female offspring (Figures S7C and S7F). Thus, the offspring of mPRε-deficient mothers exhibited metabolic dysfunction related to leanness.

Adipose mPRε exerts insulin resistance via prostaglandin production

Intracellular signaling related to adipose mPRε-mediated insulin resistance was also investigated. RNA sequencing and Kyoto Encyclopedia of Genes and Genomes (KEGG) enrichment analyses compared the WATs of WT GD16.5 and non-pregnant female mice. The results revealed a relationship between the prostaglandin synthesis pathway, chronic inflammation, and insulin resistance-related pathways, which were not observed in the WATs of mPRε-deficient mice (Figures 5A–5D) or in the livers (Figures S8A and S8B). Similarly, lipid metabolome profiling of WAT in WT GD16.5 and non-pregnant female mice revealed significant alterations in lipid mediators and polyunsaturated fatty acids, which are related to inflammation and insulin resistance (Figure 5E). Moreover, quantitative analysis revealed that prostaglandin E_2 (PGE_2) and arachidonic acid levels in the WATs of mPRε-deficient GD16.5 females were significantly lower than in WT GD16.5 females (Figure 5F). Prostaglandins via the arachidonic acid cascade are considered lipid mediators of the inflammatory response that promote insulin resistance in WAT.[34,35]

Considering that mPRβ influences the release of fatty acids from membrane phospholipids,[27] the profiles of membrane phospholipids in the WATs of pregnant and non-pregnant female mice were compared. Within the WAT membrane phospholipids of WT pregnant female mice, phosphatidylserine exhibited decreased high-carbon-chain fatty acids and increased low-carbon-chain fatty acids. This was not observed in mPRε-deficient mice (Figures S9A and S10). Additionally, phospholipase A_2 (PLA_2) activity in the WAT of mPRε-deficient GD16.5 females was significantly lower than in WT GD16.5 females (Figure S9B).

Additionally, the effects of progesterone on the mPRε-mediated release of fatty acids from membrane phospholipids in the heterologous expression system were evaluated. Similar to reports on other mPR subtypes,[27] in HEK293 cells expressing mouse mPRε, phosphorylation of ERK by progesterone was increased; similar effects were not observed in other GPCR signaling pathways such as intracellular cyclic AMP concentration (Figures S11A–S11C). Moreover, progesterone significantly enhanced PLA_2 activity in mPRε-overexpressing HEK293 cells, whereas these effects were not observed in doxycycline-uninduced control (Dox (−)), non-mPRε-expressing HEK293 cells (Figure S9C). Additionally, progesterone stimulation increased arachidonic acid levels in mPRε-overexpressing HEK293 cells, whereas these effects were not observed in Dox (−) control HEK293 cells (Figure 5G). Thus, mPRε activation by progesterone in WATs may promote PGE_2 synthesis by releasing arachidonate from phospholipids, increasing insulin resistance.

Finally, glucose tolerance tests were performed to clarify whether progesterone-induced PGE_2 production via mPRε in WATs directly causes adipose insulin resistance. Progesterone injection immediately increased arachidonate and PGE_2 levels in the WAT of WT non-pregnant female mice (Figure 6A). However, pretreating the mice with ibuprofen, as a cyclooxygenase 2 inhibitor,[36] suppressed adipose PGE_2 production (Figure 6A), preventing progesterone-induced insulin resistance (Figure 6B). In contrast, progesterone injection did not increase the arachidonate or PGE_2 levels in the WAT of mPRε-deficient non-pregnant female mice (Figure 6A), and progesterone-induced adipose insulin resistance was not observed (Figure 6B). Thus, progesterone promotes arachidonate and PGE_2 production via adipose mPRε, suppressing insulin sensitivity.

DISCUSSION

In this study, mPRε, significantly expressed in the WAT, enhanced adipose insulin resistance by inducing prostaglandin production via arachidonate release from membrane phospholipids following progesterone-stimulated PLA_2 activation. This

(D and F) Insulin tolerance test (ITT) in male (D) or female (F) WT and *mPRε*$^{-/-}$ mice was performed at 15 min post-progesterone s.c. injection. $n = 7–10$; $^{*}p < 0.05$; $^{**}p < 0.01$ vs. WT (P4, progesterone). $^{*}p < 0.05$, $^{**}p < 0.01$ (Student's t test).

(G) Insulin-stimulated Akt phosphorylation at Ser473 in the WATs, liver, and muscles of WT mice after a 5-h fast.

(H) Inhibitory effects of progesterone on insulin signaling. After pretreatment with or without progesterone (5 mg/kg, s.c.) for 30 min, a bolus of insulin (0.5 U/kg, intraperitoneally) was administered. Akt phosphorylation at Ser473 in WAT of WT mice after a 5-h fast ($n = 7–9$). $^{*}p < 0.05$; $^{**}p < 0.01$ (Dunn's post hoc test).

(I) Effect of progesterone on glucose uptake in MEF-derived adipocytes from WT or *mPRε*$^{-/-}$ mice. Glucose uptake was determined by measuring 2-deoxyglucose uptake using an enzymatic photometric assay; $n = 4$ (P4, progesterone); $^{*}p < 0.05$; $^{**}p < 0.01$ (Dunn's post hoc test). The results are presented as mean ± SEM. NS, not significant.

See also Figures S1, S2, and S3.

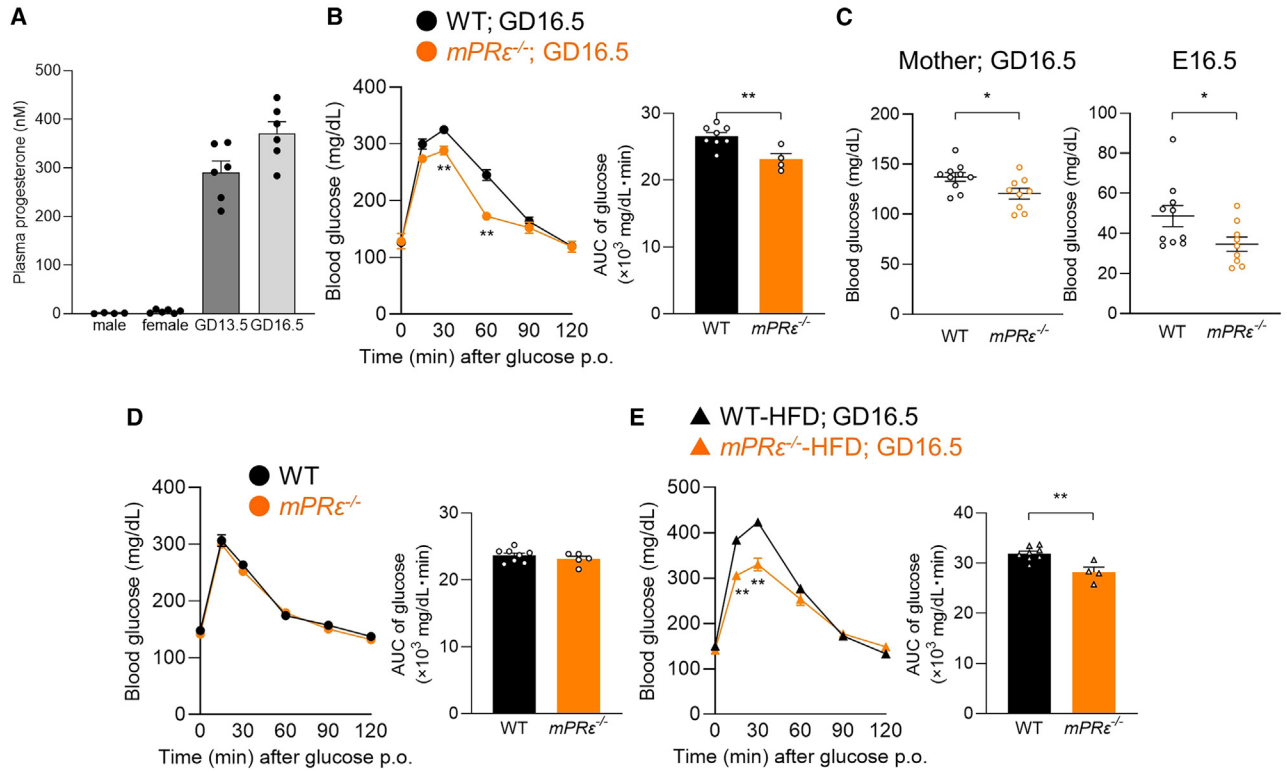

Figure 3. Maternal progesterone-adipose mPRε controls blood glucose in embryos

(A) Plasma progesterone levels in mice (male, non-pregnant, GD13.5, and GD16.5 pregnant female mice) (n = 4–6).

(B) OGTT in WT and $mPR\varepsilon^{-/-}$ GD16.5 female mice; n = 4–8; $^{**}p < 0.01$ vs. WT.

(C) Blood glucose levels in WT and $mPR\varepsilon^{-/-}$ GD16.5 female mice (left) and E16.5 embryos (right); n = 9–10; $^{*}p < 0.05$ vs. WT.

(D) OGTT in non-pregnant female mice; n = 5–8.

(E) OGTT in HFD-induced gestational diabetes mellitus model WT and $mPR\varepsilon^{-/-}$ GD16.5 female mice; n = 4–8. p.o., *per os*. $^{**}p < 0.01$ vs. WT. $^{*}p < 0.05$; $^{**}p < 0.01$ (Mann-Whitney U test). Results are presented as mean ± SEM.

See also Figures S4 and S5.

increase in maternal insulin resistance caused by the interaction between progesterone and adipose mPRε during pregnancy regulated glucose provision to embryos and offspring growth after birth.

The role of progesterone in adipocytes appears to depend on mPRε because it is abundantly expressed only in the WAT of male and female mice in mPR subtypes. Although the nuclear progesterone receptor was also expressed in WATs, expression was exclusively localized in the SVF in females. Moreover, progesterone injection increased insulin resistance via mPRε in male and female mice, suggesting that mPRε may have important functions regardless of sex. Progesterone, not estrogen, is a precursor of all steroids in the steroid biosynthetic pathway[17]; therefore, under certain physiological conditions, progesterone concentrations may become locally and temporarily elevated regardless of sex. Alternatively, given that mPRα binds to various steroids, albeit with lower affinity than with progesterone,[37] mPRε also may be activated by steroid metabolites other than progesterone.

mPRε affects energy metabolism via the liver and pancreas.[28,29] Therefore, the presence of mPRε in tissues other than WAT during pregnancy, such as the liver and pancreas, may also influence maternal insulin sensitivity. However, the results of the present study showed that progesterone injection suppressed Akt phosphorylation related to the insulin signaling pathway in WATs, not the liver or muscles, and did not affect plasma insulin levels. Moreover, in pregnancy, mPRε deficiency did not affect maternal plasma insulin levels, and RNA sequencing showed that the expressions of genes related to lipid, glucose, and energy metabolism in the liver were comparable between WT and mPRε-deficient pregnant female mice. However, progesterone in pregnancy may induce responses, other than blood glucose control, via mPRε between the mother and embryo that may involve other receptors. Hence, further studies are required to characterize the progesterone-induced maternal-fetal interactions.

The offspring from mPRε-deficient mothers exhibited leanness under HFD feeding in this study. This may be partly due to low birth weights caused by decreased glucose provision to embryos through maternal increased insulin sensitivity. Indeed, low birth weight leads to metabolic dysfunctions such as obesity or other symptoms related to leanness during development.[3–12] However, the underlying mechanism(s) remains unclear. The results of the present study suggest that variations in maternal

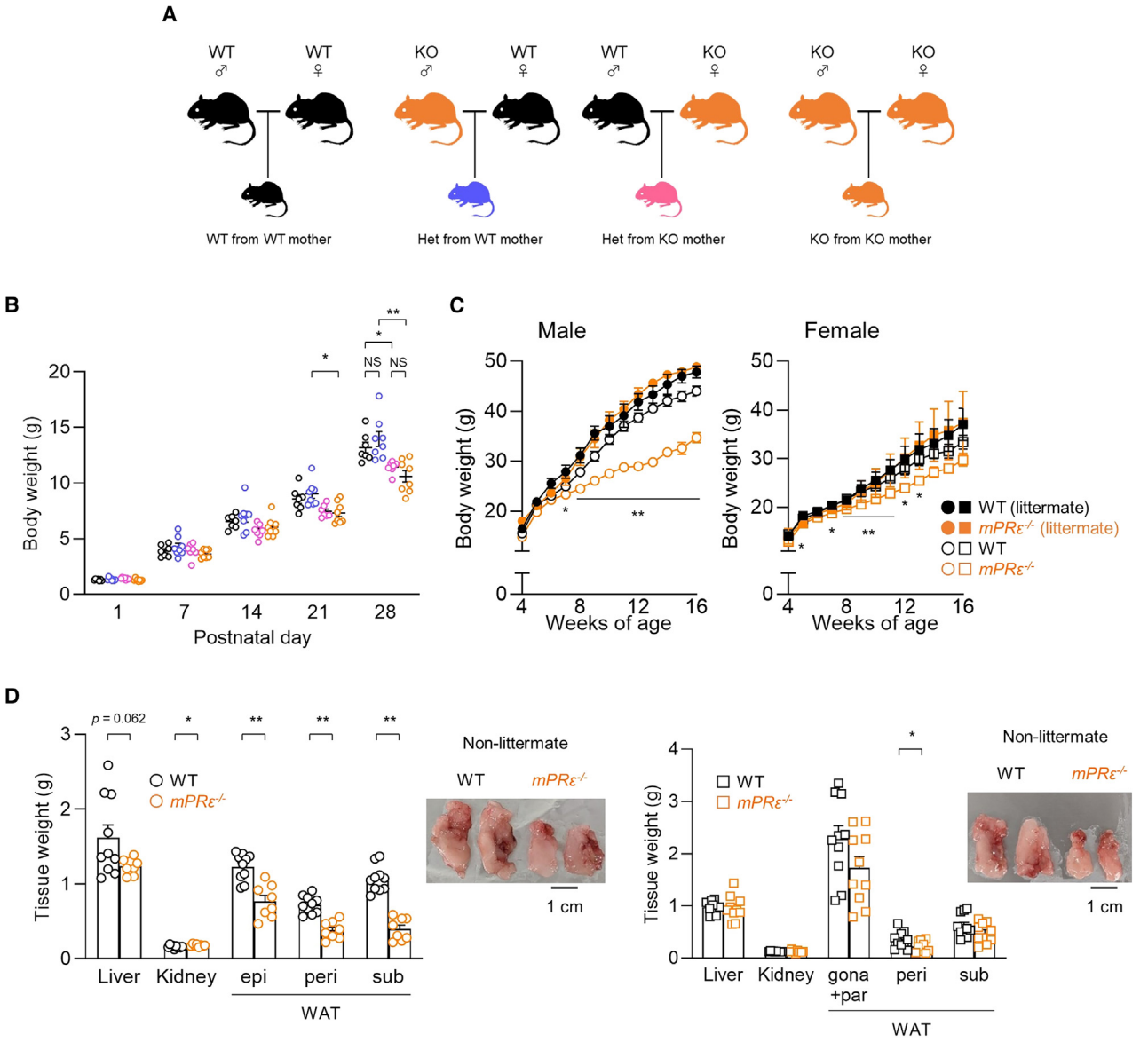

Figure 4. Offspring from mPRε-deficient female mice exhibits metabolic dysfunctions

(A) Experimental scheme.

(B) Body weight change during the growth of offspring from homozygous crosses or heterozygous crosses; $n = 7–8$. $^{*}p < 0.05$; $^{**}p < 0.01$ (Dunn's post hoc test).

(C) Changes in body weight of WT and $mPR\varepsilon^{-/-}$ offspring mice under HFD feeding in males (left) or females (right); $n = 4–10$. $^{*}p < 0.05$; $^{**}p < 0.01$ (Mann-Whitney *U* test).

(D) Tissue weights of 16-week-old $mPR\varepsilon^{-/-}$ offspring mice under HFD feeding in males (left) or females (right); $n = 8–10$. Scale bar, 1 cm. $^{*}p < 0.05$; $^{**}p < 0.01$ (Mann-Whitney *U* test). Results are presented as mean ± SEM.

See also Figures S6 and S7.

progesterone levels during pregnancy may modulate the optimal concentration of embryonic blood glucose, leading to metabolic phenotypes in offspring. Nevertheless, further studies are required to clarify the impact of longitudinal maternal glycemic control during pregnancy on the development of embryos and offspring growth.

Progesterone-induced activation of mPRε promotes intracellular PGE_2 and arachidonate production. This progesterone-mPRε-mediated response may be caused by the release of arachidonate from phospholipids via PLA_2 activity. Similarly, mPRβ is reportedly associated with PLA_2 activity.[27] The current lipid metabolome analyses revealed increased levels of other fatty acids and arachidonate in WATs during pregnancy. These results suggest that glucose and NEFAs may be efficiently supplied to embryos via adipose mPRε activation. However, further studies are warranted to clarify the

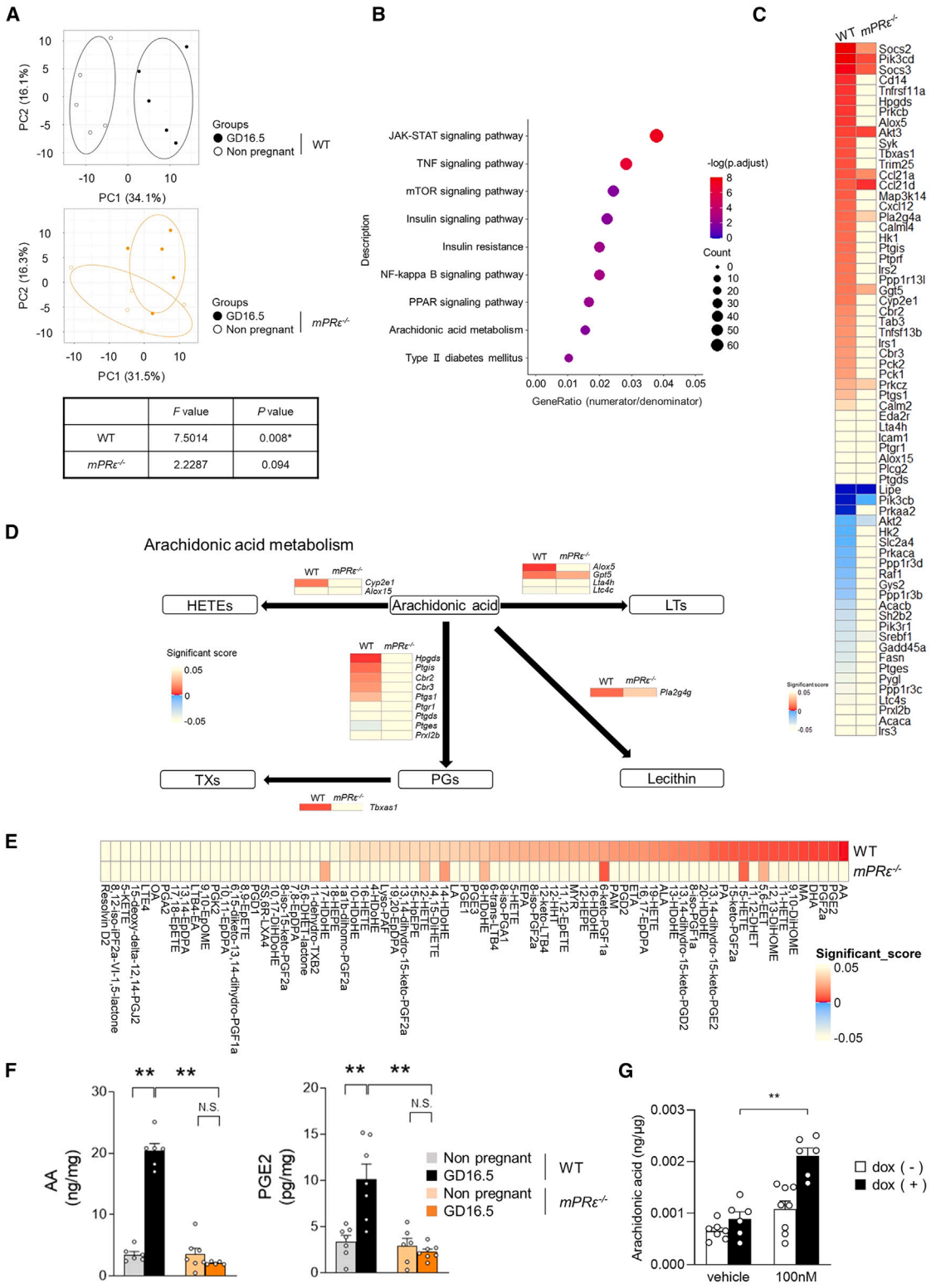

	F value	*P* value
WT	7.5014	0.008*
mPRε$^{-/-}$	2.2287	0.094

Figure 5. Prostaglandin production is increased during pregnancy via mPRε in WATs

(A) Beta diversity via the principal-component analysis (PCA) based on genes from KEGG (ID: mmu00590, mmu04064, and mmu04910) in the WATs of WT and *mPRε*$^{-/-}$ mice with non-pregnant or GD16.5; $n = 5$. Compositional similarity was compared using the permutational multivariate analysis of variance.

(B) KEGG enrichment analysis related to molecular function in WATs of GD16.5 *mPRε*$^{-/-}$ females. *p* values adjusted based on the false discovery rate (FDR).

(legend continued on next page)

progesterone-mPRε-mediated intracellular signaling mechanism as well as the specific interaction between mPRβ and PLA_2 activity.

In conclusion, this study suggests that adipose mPRε is activated by high concentrations of maternal progesterone during pregnancy, increasing maternal insulin resistance and ensuring the efficient provision of glucose to embryos. Dysfunctional maternal blood glucose control in pregnancy can lead to low birth weight or macrosomia, thereby increasing the risk of metabolic diseases in offspring during development. These results have implications for the development of mPRε-targeting drugs to selectively treat metabolic diseases without targeting progesterone.

Limitations of the study

While we used mPRε-deficient mice to investigate the role of mPRε in metabolic regulation, we did not employ tissue-specific knockouts. Therefore, the observed effects may reflect systemic rather than tissue-specific mechanisms, limiting our ability to determine the precise contributions of individual tissues, such as WATs, to the metabolic phenotypes observed. Moreover, our study primarily relied on murine models, which are valuable for investigating mechanistic pathways but may not fully recapitulate human physiology. The extent to which our findings translate to human metabolic regulation remains uncertain, and further validation in human-relevant models is necessary. Additionally, while we examined metabolic outcomes in offspring, we did not comprehensively assess how early-life metabolic phenotypes influence long-term health trajectories. In particular, the lack of longitudinal data limits our ability to establish causal relationships between maternal mPRε activity and metabolic disease risk later in life. Finally, although we used a gestational diabetes mellitus model to study maternal insulin resistance, we did not directly evaluate the metabolic characteristics of the offspring in detail. This gap raises questions regarding how maternal mPRε deficiency affects offspring metabolism beyond its effect on maternal glucose regulation.

RESOURCE AVAILABILITY

Lead contact

Further information and requests for resources and reagents should be directed to and will be fulfilled by the lead contact, Ikuo Kimura (kimura.ikuo.7x@kyoto-u.ac.jp).

Materials availability

The cells and mice generated in this study are available upon request.

Data and code availability

- All data supporting the findings of this study are available within the article and its supplemental information. Source data, including images, have been deposited in DRYAD: https://doi.org/10.5061/dryad.280gb5mzf and the DNA DataBank of Japan: E-GEAD-852, E-GEAD-853, E-GEAD-854, and E-GEAD-894.
- This paper does not report original code.
- Any additional information required to reanalyze the data reported in this paper is available from the lead contact upon request.

ACKNOWLEDGMENTS

This work was supported by research grants from the AMED (JP23gm1510011 to I.K.) and JST-MOONSHOOT (JPMJMS2023 to I.K. and J.A.). The schematics in this paper were generated using BioRender.

AUTHOR CONTRIBUTIONS

Investigation, K.W., M.Y., J.M., R.O.-K., Y. Masujima, D.S., Y. Mouri, N.K., F.O., and Y.S.; data interpretation, J.M., R.O.-K., Y. Masujima, S.I., K.N., J.A., H.O., E.K., and I.K.; writing – original draft, K.W., M.Y., and I.K.; writing – review & editing, I.K.; funding acquisition, J.A., and I.K.; supervision, I.K.

DECLARATION OF INTERESTS

D.S. is an employee of Noster, Inc.

STAR★METHODS

Detailed methods are provided in the online version of this paper and include the following:

- KEY RESOURCES TABLE
- EXPERIMENTAL MODEL AND STUDY PARTICIPANT DETAILS
  - Animal study
  - Adipocytes culture
  - Generation of HEK293 cells expressing mouse mPRε
- METHOD DETAILS
  - RNA extraction and real-time quantitative RT-PCR
  - Biochemical analyses
  - Steroid measurement
  - Insulin sensitivity analysis
  - Western blotting
  - Plasma glucose measurement
  - RNA sequencing
  - Fatty acids measurement
  - Comprehensive analysis of lipid mediators
  - Phospholipid measurement
  - PLA_2 activity in WAT
- QUANTIFICATION AND STATISTICAL ANALYSIS

(C) Heatmap of prostaglandin synthesis pathway, chronic inflammation, insulin resistance-related gene profiles of the WATs from WT and *mPRε*$^{-/-}$ non-pregnant or GD16.5 female mice; $n = 5$. Among non-pregnant vs. GD16.5 females, 66 identified genes are differentially expressed (absolute log2 fold change >0.5, $p < 0.05$: red open square).
(D) KEGG pathway analysis related to arachidonic acid metabolism in WATs of WT and *mPRε*$^{-/-}$ GD16.5 females. p values were adjusted based on the FDR.
(E) Comprehensive analysis of lipid mediators in WATs of WT and *mPRε*$^{-/-}$ GD16.5 females; heatmap of the top 40% relative lipid metabolite profiles of the WATs of WT and *mPRε*$^{-/-}$ non-pregnant or GD16.5 female mice ($n = 5$). Among non-pregnant vs. GD16.5 females, 75 genes were differentially expressed (absolute log2 fold change >0.5, $p < 0.05$: red open square).
(F) Arachidonic acid (AA, left) and PGE_2 (right) in the WATs of non-pregnant or GD16.5 females ($n = 6$–7 per group for arachidonic acid; $n = 5$–7 per group for PGE_2). $^{**}p < 0.01$ (Dunn's post hoc test).
(G) Arachidonic acid levels in response to progesterone (100 nM) in Flp-In mPRε T-REx HEK293 cells; $n = 6$–8. Cells were induced mPRε expression by treatment with doxycycline (Dox; 10 μg/mL) for 24 h.$^{**}p < 0.01$ (Mann-Whitney U test). The results are presented as mean ± SEM.
See also Figures S8, S9, S10, and S11.

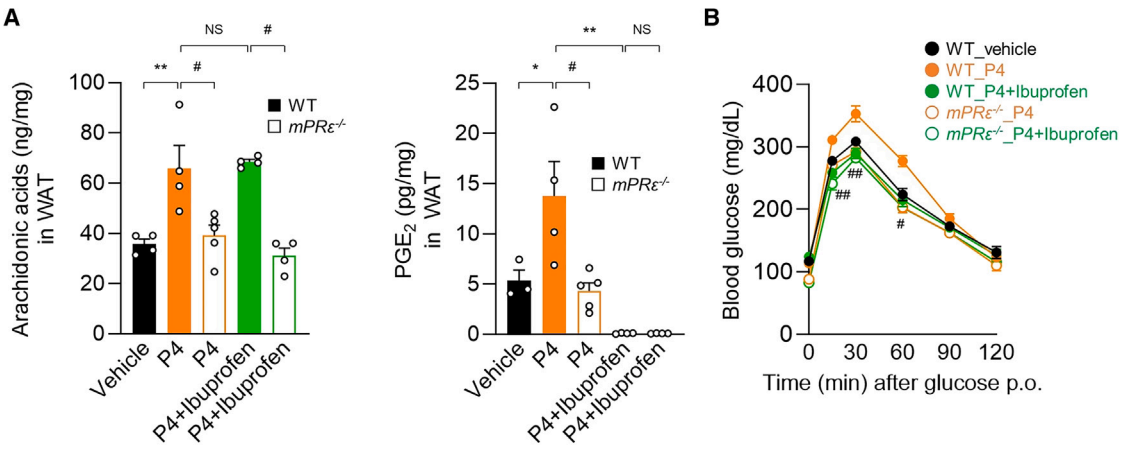

Figure 6. Progesterone-induced activation of mPRε increases insulin resistance via adipose PGE_2 production

(A) Arachidonic acid (left) and PGE_2 (right) levels in the WAT of WT and $mPR\varepsilon^{-/-}$ female mice; 15 min after s.c. progesterone injection, mice are treated with or without ibuprofen (100 mg/kg) (n = 4–5 per group for arachidonic acid; n = 3–5 per group for PGE_2). $^{*}p < 0.05$; $^{**}p < 0.01$ (Dunn's post hoc); $^{\#}p < 0.05$ (Mann-Whitney U test).

(B) OGTT in WT and $mPR\varepsilon^{-/-}$ female mice was performed at 15 min post-progesterone s.c. injection with or without ibuprofen (100 mg/kg); n = 4–5. P4, progesterone. $^{\#}p < 0.05$, $^{\#\#}p < 0.01$ between WT_P4 and WT_P4+ibuprofen (Dunn's post hoc test).

SUPPLEMENTAL INFORMATION

Supplemental information can be found online at https://doi.org/10.1016/j.celrep.2025.115433.

Received: September 4, 2024
Revised: January 21, 2025
Accepted: February 24, 2025

REFERENCES

1. Gaillard, R., and Jaddoe, V.W.V. (2023). Maternal cardiovascular disorders before and during pregnancy and offspring cardiovascular risk across the life course. Nat. Rev. Cardiol. *20*, 617–630. https://doi.org/10.1038/s41569-023-00869-z.
2. Sandovici, I., Fernandez-Twinn, D.S., Hufnagel, A., Constância, M., and Ozanne, S.E. (2022). Sex differences in the intergenerational inheritance of metabolic traits. Nat. Metab. *4*, 507–523. https://doi.org/10.1038/s42255-022-00570-4.
3. Bar-Sadeh, B., Rudnizky, S., Pnueli, L., Bentley, G.R., Stöger, R., Kaplan, A., and Melamed, P. (2020). Unravelling the role of epigenetics in reproductive adaptations to early-life environment. Nat. Rev. Endocrinol. *16*, 519–533. https://doi.org/10.1038/s41574-020-0370-8.
4. Kimura, I., Miyamoto, J., Ohue-Kitano, R., Watanabe, K., Yamada, T., Onuki, M., Aoki, R., Isobe, Y., Kashihara, D., Inoue, D., et al. (2020). Maternal gut microbiota in pregnancy influences offspring metabolic phenotype in mice. Science *367*, eaaw8429. https://doi.org/10.1126/science.aaw8429.
5. Lopez-Tello, J., Yong, H.E.J., Sandovici, I., Dowsett, G.K.C., Christoforou, E.R., Salazar-Petres, E., Boyland, R., Napso, T., Yeo, G.S.H., Lam, B.Y.H., et al. (2023). Fetal manipulation of maternal metabolism is a critical function of the imprinted Igf2 gene. Cell Metab. *35*, 1195–1208.e6. https://doi.org/10.1016/j.cmet.2023.06.007.
6. Bentley-Lewis, R., Levkoff, S., Stuebe, A., and Seely, E.W. (2008). Gestational diabetes mellitus: postpartum opportunities for the diagnosis and prevention of type 2 diabetes mellitus. Nat. Clin. Pract. Endocrinol. Metab. *4*, 552–558. https://doi.org/10.1038/ncpendmet0965.
7. Wadhwa, P.D., Buss, C., Entringer, S., and Swanson, J.M. (2009). Developmental origins of health and disease: brief history of the approach and current focus on epigenetic mechanisms. Semin. Reprod. Med. *27*, 358–368. https://doi.org/10.1055/s-0029-1237424.
8. Parlee, S.D., and MacDougald, O.A. (2014). Maternal nutrition and risk of obesity in offspring: the Trojan horse of developmental plasticity. Biochim. Biophys. Acta *1842*, 495–506. https://doi.org/10.1016/j.bbadis.2013.07.007.
9. Whitaker, R.C., Wright, J.A., Pepe, M.S., Seidel, K.D., and Dietz, W.H. (1997). Predicting obesity in young adulthood from childhood and parental obesity. N. Engl. J. Med. *337*, 869–873. https://doi.org/10.1056/NEJM199709253371301.
10. Binkin, N.J., Yip, R., Fleshood, L., and Trowbridge, F.L. (1988). Birth weight and childhood growth. Pediatrics *82*, 828–834. https://doi.org/10.1542/peds.82.6.828.
11. Harder, T., Rodekamp, E., Schellong, K., Dudenhausen, J.W., and Plagemann, A. (2007). Birth weight and subsequent risk of type 2 diabetes: a meta-analysis. Am. J. Epidemiol. *165*, 849–857. https://doi.org/10.1093/aje/kwk071.
12. Nam, H.K., and Lee, K.H. (2018). Small for gestational age and obesity: epidemiology and general risks. Ann. Pediatr. Endocrinol. Metab. *23*, 9–13. https://doi.org/10.6065/apem.2018.23.1.9.
13. O'Malley, B.W., and Means, A.R. (1974). Female steroid hormones and target cell nuclei. Science *183*, 610–620. https://doi.org/10.1126/science.183.4125.610.
14. Drury, E.R., Wu, J., Gigliotti, J.C., and Le, T.H. (2024). Sex differences in blood pressure regulation and hypertension: renal, hemodynamic, and hormonal mechanisms. Physiol. Rev. *104*, 199–251. https://doi.org/10.1152/physrev.00041.2022.
15. Saunders, F.J. (1968). Effects of sex steroids and related compounds on pregnancy and on development of the young. Physiol. Rev. *48*, 601–643. https://doi.org/10.1152/physrev.1968.48.3.601.
16. López-García, C., López-Contreras, A.J., Cremades, A., Castells, M.T., Marín, F., Schreiber, F., and Peñafiel, R. (2008). Molecular and morphological changes in placenta and embryo development associated with the inhibition of polyamine synthesis during midpregnancy in mice. Endocrinology *149*, 5012–5023. https://doi.org/10.1210/en.2008-0084.
17. Losel, R.M., Falkenstein, E., Feuring, M., Schultz, A., Tillmann, H.C., Rossol-Haseroth, K., and Wehling, M. (2003). Nongenomic steroid action: controversies,

questions, and answers. Physiol. Rev. *83*, 965–1016. https://doi.org/10.1152/physrev.00003.2003.

18. Garg, D., Ng, S.S.M., Baig, K.M., Driggers, P., and Segars, J. (2017). Progesterone-Mediated Non-Classical Signaling. Trends Endocrinol. Metab. *28*, 656–668. https://doi.org/10.1016/j.tem.2017.05.006.
19. Prossnitz, E.R., and Barton, M. (2011). The G-protein-coupled estrogen receptor GPER in health and disease. Nat. Rev. Endocrinol. *7*, 715–726. https://doi.org/10.1038/nrendo.2011.122.
20. Thomas, P. (2008). Characteristics of membrane progestin receptor alpha (mPRalpha) and progesterone membrane receptor component 1 (PGMRC1) and their roles in mediating rapid progestin actions. Front. Neuroendocrinol. *29*, 292–312. https://doi.org/10.1016/j.yfrne.2008.01.001.
21. Kasubuchi, M., Watanabe, K., Hirano, K., Inoue, D., Li, X., Terasawa, K., Konishi, M., Itoh, N., and Kimura, I. (2017). Membrane progesterone receptor beta (mPRβ/Paqr8) promotes progesterone-dependent neurite outgrowth in PC12 neuronal cells via non-G protein-coupled receptor (GPCR) signaling. Sci. Rep. *7*, 5168. https://doi.org/10.1038/s41598-017-05423-9.
22. Gonzalez-Velazquez, W., Gonzalez-Mendez, R., and Rodriguez-del Valle, N. (2012). Characterization and ligand identification of a membrane progesterone receptor in fungi: existence of a novel PAQR in Sporothrix schenckii. BMC Microbiol. *12*, 194. https://doi.org/10.1186/1471-2180-12-194.
23. Lyons, T.J., Villa, N.Y., Regalla, L.M., Kupchak, B.R., Vagstad, A., and Eide, D.J. (2004). Metalloregulation of yeast membrane steroid receptor homologs. Proc. Natl. Acad. Sci. USA *101*, 5506–5511. https://doi.org/10.1073/pnas.0306324101.
24. Tang, Y.T., Hu, T., Arterburn, M., Boyle, B., Bright, J.M., Emtage, P.C., and Funk, W.D. (2005). PAQR proteins: a novel membrane receptor family defined by an ancient 7-transmembrane pass motif. J. Mol. Evol. *61*, 372–380. https://doi.org/10.1007/s00239-004-0375-2.
25. Zhu, Y., Bond, J., and Thomas, P. (2003). Identification, classification, and partial characterization of genes in humans and other vertebrates homologous to a fish membrane progestin receptor. Proc. Natl. Acad. Sci. USA *100*, 2237–2242. https://doi.org/10.1073/pnas.0436133100.
26. Smith, J.L., Kupchak, B.R., Garitaonandia, I., Hoang, L.K., Maina, A.S., Regalla, L.M., and Lyons, T.J. (2008). Heterologous expression of human mPRalpha, mPRbeta and mPRgamma in yeast confirms their ability to function as membrane progesterone receptors. Steroids *73*, 1160–1173. https://doi.org/10.1016/j.steroids.2008.05.003.
27. Nader, N., Assaf, L., Zarif, L., Halama, A., Yadav, S., Dib, M., Attarwala, N., Chen, Q., Suhre, K., Gross, S., and Machaca, K. (2024). Progesterone induces meiosis through two obligate co-receptors with PLA2 activity. Elife *13*, RP92635. https://doi.org/10.7554/eLife.92635.
28. Lin, Y., Chen, L., You, X., Li, Z., Li, C., and Chen, Y. (2021). PAQR9 regulates hepatic ketogenesis and fatty acid oxidation during fasting by modulating protein stability of PPARα. Mol. Metab. *53*, 101331. https://doi.org/10.1016/j.molmet.2021.101331.
29. Li, Z., Lin, Y., Zhuo, S., Chen, J., Chen, L., Wang, S., and Chen, Y. (2023). PAQR9 regulates glucose homeostasis in diabetic mice and modulates insulin secretion in β cells in vitro under stress conditions. Mol. Cell. Endocrinol. *575*, 112032. https://doi.org/10.1016/j.mce.2023.112032.
30. Hilliad, J. (1973). Corpus luteum function in guinea pigs, hamsters, rats, mice and rabbits. Biol. Reprod. *8*, 203–221. https://doi.org/10.1093/biolreprod/8.2.203.
31. Kimura, I., Ozawa, K., Inoue, D., Imamura, T., Kimura, K., Maeda, T., Terasawa, K., Kashihara, D., Hirano, K., Tani, T., et al. (2013). The gut microbiota suppresses insulin-mediated fat accumulation via the short-chain fatty acid receptor GPR43. Nat. Commun. *4*, 1829. https://doi.org/10.1038/ncomms2852.
32. Kampmann, U., Ovesen, P.G., Møller, N., and Fuglsang, J. (2021). Extreme insulin resistance during pregnancy: a therapeutic challenge. Endocrinol Diabetes Metab Case Rep *2021*, 20–0191. https://doi.org/10.1530/EDM-20-0191.
33. Kramer, A.C., Jansson, T., Bale, T.L., and Powell, T.L. (2023). Maternal-fetal cross-talk via the placenta: influence on offspring development and metabolism. Development *150*, dev202088. https://doi.org/10.1242/dev.202088.
34. Buckley, C.D., Gilroy, D.W., and Serhan, C.N. (2014). Proresolving lipid mediators and mechanisms in the resolution of acute inflammation. Immunity *40*, 315–327. https://doi.org/10.1016/j.immuni.2014.02.009.
35. Chan, P.C., Hsiao, F.C., Chang, H.M., Wabitsch, M., and Hsieh, P.S. (2016). Importance of adipocyte cyclooxygenase-2 and prostaglandin E2-prostaglandin E receptor 3 signaling in the development of obesity-induced adipose tissue inflammation and insulin resistance. FASEB J. *30*, 2282–2297. https://doi.org/10.1096/fj.201500127.
36. Mallet, C., Barrière, D.A., Ermund, A., Jönsson, B.A.G., Eschalier, A., Zygmunt, P.M., and Högestätt, E.D. (2010). TRPV1 in brain is involved in acetaminophen-induced antinociception. PLoS One *5*, e12748. https://doi.org/10.1371/journal.pone.0012748.
37. Thomas, P., Pang, Y., Dong, J., Groenen, P., Kelder, J., de Vlieg, J., Zhu, Y., and Tubbs, C. (2007). Steroid and G protein binding characteristics of the seatrout and human progestin membrane receptor alpha subtypes and their evolutionary origins. Endocrinology *148*, 705–718. https://doi.org/10.1210/en.2006-0974.
38. Bolger, A.M., Lohse, M., and Usadel, B. (2014). Trimmomatic: a flexible trimmer for Illumina sequence data. Bioinformatics *30*, 2114–2120. https://doi.org/10.1093/bioinformatics/btu170.
39. Cock, P.J.A., Fields, C.J., Goto, N., Heuer, M.L., and Rice, P.M. (2010). The Sanger FASTQ file format for sequences with quality scores, and the Solexa/Illumina FASTQ variants. Nucleic Acids Res. *38*, 1767–1771. https://doi.org/10.1093/nar/gkp1137.
40. Dobin, A., Davis, C.A., Schlesinger, F., Drenkow, J., Zaleski, C., Jha, S., Batut, P., Chaisson, M., and Gingeras, T.R. (2013). STAR: ultrafast universal RNA-seq aligner. Bioinformatics *29*, 15–21. https://doi.org/10.1093/bioinformatics/bts635.
41. Li, B., and Dewey, C.N. (2011). RSEM: accurate transcript quantification from RNA-Seq data with or without a reference genome. BMC Bioinf. *12*, 323. https://doi.org/10.1186/1471-2105-12-323.
42. Lee, M.L., Matsunaga, H., Sugiura, Y., Hayasaka, T., Yamamoto, I., Ishimoto, T., Imoto, D., Suematsu, M., Iijima, N., Kimura, K., et al. (2021). Prostaglandin in the ventromedial hypothalamus regulates peripheral glucose metabolism. Nat. Commun. *12*, 2330. https://doi.org/10.1038/s41467-021-22431-6.
43. BLIGH, E.G., and DYER, W.J. (1959). A rapid method of total lipid extraction and purification. Can. J. Biochem. Physiol. *37*, 911–917. https://doi.org/10.1139/o59-099.
44. Murate, M., Yokoyama, N., Tomishige, N., Richert, L., Humbert, N., Pollet, B., Makino, A., Kono, N., Mauri, L., Aoki, J., et al. (2023). Cell density-dependent membrane distribution of ganglioside GM3 in melanoma cells. Cell. Mol. Life Sci. *80*, 167. https://doi.org/10.1007/s00018-023-04813-9.

STAR★METHODS

KEY RESOURCES TABLE

REAGENT or RESOURCE	SOURCE	IDENTIFIER
Antibodies		
Akt	Cell Signaling Technology	Cat# 4691S; RRID: AB_915783
phosphorylated Akt	Cell Signaling Technology	Cat# 9271S; RRID: AB_329825
ERK	Cell Signaling Technology	Cat# 9102S; RRID: AB_330744
phosphorylated ERK	Cell Signaling Technology	Cat# 9101S; RRID: AB_331646
horseradish peroxidase-conjugated donkey anti-rabbit antibody	Cell Signaling Technology	Cat# NA934V; RRID: AB_772206
Critical commercial assays		
RNeasy Mini Kit	Qiagen	Cat# 74106
SYBR Premix Ex Taq II	TAKARA	Cat# RR820B
LabAssay™ NEFA	FUJIFILM Wako Pure Chemical Corporation	Cat# 294-63601
LabAssay™ Triglyceride	FUJIFILM Wako Pure Chemical Corporation	Cat# 290-63701
LabAssay™ Cholesterol	FUJIFILM Wako Pure Chemical Corporation	Cat# 294-65801
[insulin enzyme-linked immunosorbent assay (ELISA) kit (RTU)	Shibayagi	Cat# AKRIN-011RU
2-deoxyglucose (2DG) Uptake Measurement kit	Cosmo Bio	Cat# OKP-PMG-K01
Agilent 2100 Bioanalyzer system with an RNA 6000 Nano Kit	Agilent Technologies	Cat# 5067-1511
NEBNext® Ultra™ II Directional RNA Library Prep Kit	Illumina	Cat# E7760L
NEBNext Multiplex Oligos for Illumina (Dual Index Primers Set 1)	Illumina	Cat# E7600S
cPLA2 Assay Kit	Cayman Chemical	Cat# 765021
cAMP EIA kit	Cayman Chemical	Cat# 581002
Deposited data		
Raw files for RNA-seq	This paper	E-GEAD-852, E-GEAD-853, E-GEAD-854, and E-GEAD-894
Source data presented	This paper	https://doi.org/10.5061/dryad.280gb5mzf
Experimental models: Cell lines		
HEK293	ATCC	Cat# CRL-1573
Experimental models: Organisms/strains		
C57BL/6N mice	NIH	N/A
mPRε−/− mice	NIH	N/A
Oligonucleotides		
mPRε (forward) 5′-CACTTCATCCCGCTGCTGCT-3′	This paper	N/A
mPRε (reverse) 5′- GCGGCTCTTACAGCAAGCCA-3′	This paper	N/A
mPRα (forward) 5′-CGGCATGGCGATGGCAGTA-3′	This paper	N/A
mPRα (reverse) 5′-CTGCACCTTGTCATGCCAGG-3′	This paper	N/A
mPRβ (forward) 5′-CACCGCTGTGTCATGACGCT-3′	This paper	N/A
mPRβ (reverse) 5′-GCCTGGTCGGAGCTATAGA-3′	This paper	N/A
mPRγ (forward) 5′-TGACAGCTACTCGTGGCCGA-3′	This paper	N/A
mPRγ (reverse) 5′-GCCCATGTGCTTCTGGTGGT-3′	This paper	N/A
mPRδ (forward) 5′-TACTGCCCGCCTGCCTCTAT-3′	This paper	N/A

(*Continued on next page*)

Continued

REAGENT or RESOURCE	SOURCE	IDENTIFIER
mPRδ (reverse) 5′-TGAGAGCAGAGCGCAGAGGA-3′	This paper	N/A
PGR (forward) 5′-CGACGTGGAGGGAGCTTTCT-3′	This paper	N/A
PGR (reverse) 5′-CCTGGGTGGTGACAGTCCTT-3′	This paper	N/A
18S (forward) 5′-ACGCTGAGCCAGTCAGTGTA-3′	This paper	N/A
18S (reverse) 5′-CTTAGAGGGACAAGTGGCG-3′	This paper	N/A
Software and algorithms		
trimmomatic-0.39	Bolger et al.[38]	https://github.com/usadellab/Trimmomatic/releases
FastQC (version 0.11.8.-2)	Cock et al.[39]	https://github.com/s-andrews/FastQC
STAR software (version 2.7.10a)	Dobin et al.[40]	https://github.com/alexdobin/STAR/releases
RSEM (version 1.3.3)	Li et al.[41]	https://bioweb.pasteur.fr/packages/pack@RSEM@1.3.3
GraphPad Prism 10	GraphPad Software	https://www.graphpad.com/updates
R, v4.4.0	R Development Core Team, 2022	https://www.r-project.org
RStudio, v2024.04.1	RStudio: Integrated Development for R, Boston, MA	https://www.rstudio.com
Other		
High-fat diet (60% kcal of fat)	Research Diets Inc	D12492
Normal Chow Diet	CLEA Japan	CE-2

EXPERIMENTAL MODEL AND STUDY PARTICIPANT DETAILS

Animal study

Male and female C57BL/6 mice were obtained from Japan SLC (RRID: IMSR_JAX:000664, Shizuoka, Japan), whereas *mPRε*$^{-/-}$ mice with C57BL/6N background were generated. The mice were house in a conventional animal facility at 24°C with a 12 h light/dark cycle and were acclimated to the CLEA Rodent Diet (CE-2; CLEA Japan, Inc.) for 1 week before initiating treatments.

For the high fat diet (HFD) feeding study, 4-week-old mice were fed either NC or HFD with 60% kcal fat (D12492, Research Diets Inc) for 12 weeks. Body weight was recorded weekly throughout the experiment. At the end of the study, all the mice were euthanized under deep isoflurane anesthesia.

All procedures involving animals were conducted in compliance with the guidelines of the Committee on the Ethics of Animal Experiments of the Kyoto University Animal Experimentation Committee (Lif-K23012), ensuring that all efforts were made to minimize animal distress.

Adipocytes culture

Mouse embryonic fibroblast (MEF)-derived adipocytes were cultured at 37°C in α-minimum essential medium (MEM) supplemented with 1% penicillin-streptomycin solution (Gibco) and 10% fetal bovine serum (FBS). Two days after reaching confluence, the medium was replaced with α-MEM containing 10% FBS and inducers (0.25 μM dexamethasone, 10 μg/mL insulin, and 0.5 mM 3-isobutyl-1-methylxanthine [IBMX]) along with pioglitazone (10 μM) for 2 d. Subsequently, the medium was switched to Dulbecco's modified eagle medium (DMEM) supplemented with 10% FBS, 10 μg/mL insulin, and 10 μM pioglitazone for another 12 d. The fully differentiated adipocytes were then ready for experimentation.[31]

For the glucose uptake assay, MEF-derived adipocytes were incubated in a serum-free medium for 6 h and subsequently treated progesterone at 37°C for 20 min. Insulin (3 μg/mL) and 0.1 mM 2-deoxyglucose (Sigma) were then added, and the cells were incubated at 37°C for an additional 20 min. The adipocytes were washed thrice with ice-cold phosphate-buffered saline (PBS) containing phloretin and collected in 1% NP-40/10 mM Tris-HCl. The cell lysates were heat-treated at 80°C for 15 min and centrifuged at 15,000 × *g* for 20 min at 4°C. The supernatants were collected and analyzed using a 2-deoxyglucose (2DG) Uptake Measurement kit (Cosmo Bio).

For Oil Red O staining, the cells were fixed with 4% paraformaldehyde (PFA) for 10 min and washed thrice with PBS. Fixed cells were stained with Oil Red O for 10 min, washed with distilled water, and extracted with isopropanol. The absorbance at 530 nm wavelength was measured for quantitative analysis.

Generation of HEK293 cells expressing mouse mPRε

Flp-In T-REx HEK293 cells were sourced from Invitrogen. To generate HEK293 cells expressing mouse mPRε, the cells were transfected with pcDNA5/FRT/TO-E-tag-mPRε and pOG44 using Lipofectamine reagent (Invitrogen).[21] Transfected cells were cultured in DMEM supplemented with 10 μg/mL blasticidin S (Funakoshi), 100 μg/mL hygromycin B (Gibco), and 10% FBS. Before each experiment, cells were treated with or without Dox (10 μg/mL) for 24 h. The cells were maintained at 37°C in a 5% CO_2 atmosphere and cultured under various conditions.

To assess the PLA_2 activity, HEK293 cells were plated in 24-well plates (1×10^5 cells/well) and cultured for 24 h. Subsequently, each well was stimulated with progesterone for 24 h and collected in 50 mM HEPES buffer containing 1 mM EDTA (pH 7.4). The lysates were centrifuged at ×10,000 × *g* for 15 min at 4°C. The supernatants were collected, and the PLA_2 activity was measured using the $cPLA_2$ Assay Kit (Cayman Chemical) following the manufacturer's protocol. The cAMP concentration was determined by enzyme immunoassay (EIA) using a cAMP EIA kit (Cayman Chemical), following the manufacturer's protocol. For cAMP determination, the cells were lysed in a 0.1 N HCl solution.[21] All assays were conducted in duplicates.

METHOD DETAILS

RNA extraction and real-time quantitative RT-PCR

Total RNA was extracted using an RNeasy Mini Kit (Qiagen) and RNAiso Plus reagent (TAKARA). Complementary DNA (cDNA) was synthesized from the RNA templates using Moloney murine leukemia virus reverse transcriptase (Invitrogen). Quantitative reverse transcriptase PCR (qRT-PCR) was conducted using SYBR Premix Ex Taq II (TAKARA) on a StepOnePlus real-time PCR system (Applied Biosystems), following previously described protocols.[31] The PCR program was as follows: initial denaturation at 95°C for 30 s, followed by 40 cycles of 95°C for 5 s, 58°C for 30 s and 72°C for 1 min. The dissociation stage was carried out at 95°C for 15 s, followed by 60°C for 1 min, and a final step at 95°C for 15 s. Primers sequences are listed in the key resources table.

Biochemical analyses

Plasma levels of NEFA (LabAssay NEFA), triglyceride (LabAssay Triglyceride), and total cholesterol (LabAssay Cholesterol) were measured in mice following the manufacturer's protocols. Blood glucose levels were determined using a handheld glucometer (OneTouch Ultra; LifeScan). Plasma insulin levels were assessed using an insulin ELISA kit [insulin enzyme-linked immunosorbent assay (ELISA) kit (RTU)], per the manufacturer's instructions.

Steroid measurement

For steroid measurements, plasma samples were mixed with methanol containing an internal standard, followed by ethyl acetate for lipid extraction. The mixture was centrifuged at 8,000 × *g* at 4°C for 15 min, and the supernatants containing the steroids were collected and dried. Subsequently, the dried samples were redissolved in methoxyamine hydrochloride (20 mg/mL in pyridine) and incubated (60 °C, 45 min) for derivatization. The dried samples were resuspended in acetonitrile and analyzed by liquid chromatography-tandem mass spectrometry (LC–MS/MS) with an ultra-performance liquid chromatography (UPLC) system (Waters) equipped with an Acquity UPLC system coupled to a Waters Xevo TQD mass spectrometer (Waters). Separation was achieved using an acetonitrile gradient in a 0.1% formic acid aqueous solution on an Acquity UPLC BEH C18 column (2.1 × 150 mm, 1.7 μm; Waters).

Insulin sensitivity analysis

To evaluate glucose tolerance in HFD-induced obesity, mice were given an oral gavage of glucose (1.5 g/kg body weight) after a 16 h fast. Although non-pregnant mice were given an oral gavage of glucose (1.5 g/kg body weight) after a 6 h fast. To assess the insulin tolerance in HFD-induced obesity, mice were fasted for 4 h and then intraperitoneally injected with insulin (0.5 U/kg; Sigma-Aldrich, St. Louis, MO, USA). Blood glucose levels were measured before injection and at 15, 30, 60, 90, and 120 min post-injection. To assess the biochemical responses to insulin stimulation, mice treated with or without progesterone (5 mg/kg, s.c.) were injected intraperitoneally with insulin (0.5 U/kg). After 15 min, the liver, skeletal muscles, and WATs were collected and immediately frozen in liquid nitrogen. Immunoblotting was performed as previously described.[31] To assess the effect of COX-2 inhibition, mice were subcutaneously injected (s.c.) with ibuprofen (100 mg/kg) 30 min before and progesterone (5 mg/kg) 15 min before oral administration of glucose. Blood glucose levels were measured before injection and 15, 30, 60, 90, and 120 min post-injection.

Western blotting

Tissues were homogenized in 0.1 M sodium phosphate buffer (pH 7.4) and centrifuged at 14,000 × *g* for 30 min at 4°C. Tissue lysates were prepared in a TNE buffer containing 10 mM Tris-HCl (pH 7.4), 150 mM NaCl, 1 mM EDTA, 1% Nonidet P-40, 50 mM NaF, 2 mM Na_3VO_4, 10 μg/mL aprotinin, and a 1% phosphatase inhibitor cocktail (Nacalai Tesque). Proteins from the lysates were separated via sodium dodecyl sulfate-polyacrylamide gel electrophoresis and transferred to nitrocellulose membranes. Proteins were detected by western blotting using antibodies specific for Akt (1:1000; Cell Signaling Technology), phosphorylated Akt (1:1000; Cell Signaling Technology), ERK (1:1000; Cell Signaling Technology), and phosphorylated ERK (1:1000; Cell Signaling Technology). The membranes were then treated with a horseradish peroxidase-conjugated donkey anti-rabbit secondary antibody (1:2000; GE Healthcare).

Immunoreactive bands were visualized using an enhanced chemiluminescence detection system as previously described.[31] The ImageJ software (National Institutes of Health) was used to quantify the integrated density of each band.

Plasma glucose measurement

To quantify glucose in the embryo plasma, acetone was added to plasma samples, mixed using a vortex, and centrifuged at 10,000 × *g* for 5 min at 4°C. The supernatant was collected for LC–MS/MS analysis. Glucose was analyzed using an Acquity UPLC system coupled to a Waters Xevo TQD mass spectrometry (Waters) and separated on an Acquity UPLC BEH Amide column (2.1 × 150 mm, 1.7 μm; Waters) using a concentration gradient of water, acetonitrile, acetone, and 4% ammonium hydroxide.

RNA sequencing

RNA was extracted from the WAT and liver of non-pregnant and pregnant mice and placenta from pregnant mice using RNAiso Plus reagent (TAKARA) and the RNeasy Mini Kit (Qiagen). RNA integrity, quality, and concentration were measured using an Agilent 2100 Bioanalyzer system with an RNA 6000 Nano Kit (Agilent Technologies). RNA sequencing libraries were prepared using the NEBNext Ultra II Directional RNA Library Prep Kit (Illumina) and NEBNext Multiplex Oligos for Illumina (Dual Index Primers Set 1) and sequenced on an Illumina NovaSeq 6000. Each sample yielded approximately 4 Gb of paired-end reads with a length of 150 bp. The obtained RNA sequencing data were processed using trimmomatic-0.39 to eliminate adapters and low-quality reads.[38] The quality of the trimmed sequences was evaluated using FastQC (version 0.11.8.-2).[39] Alignment of the reads to the mouse reference genome (NCBI GRCm39) was performed using the STAR software (version 2.7.10a).[40] The raw read counts were subjected to relative log expression normalization to identify differentially expressed genes (DEGs) across all comparisons. Fold changes were calculated using RSEM (version 1.3.3) and edgeR.[41] DEGs were determined based on two criteria: a false discovery rate (FDR)-adjusted *p*-value <0.05 (Benjamini-Hochberg procedure) and an absolute log2 fold change >0.5. Gene Set Enrichment Analysis was performed using the Kyoto Encyclopedia of Genes and Genomes (KEGG) database (http://www.genome.jp/kegg/).

Fatty acids measurement

To quantify individual FAs, samples (approximately 50 mg adipose tissue or 1.2 × 10^6 mPRε-overexpressing HEK293 cells) were homogenized in methanol (1 mL) with an internal control (C17:1). Chloroform (2 mL) and 0.5 M potassium chloride (0.75 mL) were added to extract lipids. The collected lipid layers were dried and the samples were resuspended in chloroform:methanol (1:3, v/v) for LC–MS/MS analysis. FAs were analyzed using an Acquity UPLC system coupled to a Waters Xevo TQD mass spectrometry (Waters) and separated on an Acquity UPLC BEH C18 column (2.1 × 150 mm, 1.7 μm; Waters) using an acetonitrile gradient in 10mM ammonium formate aqueous solution. The flow rate was 0.4 mL/min, and the column temperature was maintained at 50°C. MS detection was performed in the negative ionization mode, with the source capillary voltage set to 3000 V. The desolvation and source temperatures were set at 500°C and 150°C, respectively. Individually optimized multiple reaction monitoring parameters were determined for the target compounds using standards.

Comprehensive analysis of lipid mediators

To quantify prostaglandins in tissues, solid-phase extraction was performed using Oasis HLB cartridges (1 mg; Waters), according to the method described by Lee et al.[42] Briefly, the samples were homogenized in methanol and the supernatants were diluted with water to achieve a final methanol concentration of approximately 7%. The diluted samples were applied to pretreated cartridges and sequentially washed with 0.1% formic acid, 15% ethanol, and hexane. The samples were eluted with 200 μL of methanol and dried. The dried samples were reconstituted in 20 μL of methanol and subjected to LC–MS/MS analysis. A Shimadzu LC/MS/MS Method Package for Lipid Mediators ver. 2 (Shimadzu) was used to analyze various lipid mediators. The analysis was performed on a Shimadzu LCMS-8060NX Triple Quadrupole LC–MS/MS system and separated on a Kinetex C8 column (2.1 × 150 mm, 2.6 μm; Phenomenex).

Phospholipid measurement

Total lipids in WAT samples were extracted using the method described by Bligh and Dyer.[43] The extracted lipids were dried up with a centrifugal evaporator, dissolved in methanol: isopropanol = 1:1, and stored at −20°C. Lipid samples were subjected to LC/ESI-MS-based lipidomic analyses using a Shimadzu Nexera UPLC system (Shimadzu) coupled with a QTRAP 4500 hybrid triple quadrupole linear ion trap mass spectrometer (SCIEX). Chromatographic separation was performed on a SeQuant ZIC-HILIC PEEK coated column (250 mm × 2.1 mm, 1.8 μm; Millipore) maintained at 50°C using mobile phase A (water/acetonitrile (95/5, v/v) containing 10 mM ammonium acetate) and mobile phase B (water/acetonitrile (50/50, v/v) containing 20 mM ammonium acetate) in a gradient program (0–22 min: 0% B→40% B; 22–25 min: 40% B→40% B; 25–30 min: 0% B) with a flow rate of 0.3 mL/min. Instrument parameters were as follows: curtain gas, 30 psi; collision gas, 7 arb. unit; ionspray voltage, −4500 V; temperature, 700°C; ion source gas 1, 30 psi; ion source gas 2, 70 psi. Phospholipid species were detected by multiple reaction monitoring as previously described.[44]

PLA_2 activity in WAT

WAT samples of WT and *mPRε*$^{-/-}$ GD16.5 female mice were washed with PBS containing 0.16 g/mL heparin (pH 7.4) to eliminate adhered red blood cells and clots. After removing the PBS, samples were homogenized in 50 mM HEPES containing 1 mM EDTA

buffer (pH 7.4) on ice and centrifuged at 10,000 × *g* for 15 min at 4°C. The supernatants were collected, and PLA_2 activity was measured using a phospholipase A2 calcium-dependent cytosolic assay kit ($cPLA_2$ Assay Kit, Cayman Chemical) per the manufacturer's instructions.

QUANTIFICATION AND STATISTICAL ANALYSIS

All data are expressed as the mean ± standard error of the mean (SEM). Statistical analyses were performed using GraphPad Prism software (GraphPad Software Inc.). Data normality was assessed using the Shapiro–Wilk test. Depending on the normality of the data, statistical comparisons were conducted using the Student's *t*-test (two-tailed), Mann–Whitney U test (two-tailed), or two-way ANOVA with the Bonferroni or Dunn's post hoc test. Statistical significance was defined as $p < 0.05$.